



Geospatial Auto-correlation Statistical Analysis to Evaluate the Seismic Magnitudes and Its Implications on the Mediterranean Coastal Zone of Egypt

Ali Amasha^{1*}, Islam Abou El-Magd² and Elham Ali³

¹Arab Academy for Science, Technology & Maritime Transport, Complex, Block 1167, Off El-Moshir Ahmed Ismail St., P.O.Box 2033 – El-Horria, Cairo, Egypt.

²National authority for Remote Sensing and Space Sciences, 23 Josef Tito St., El-Nozaha El-Gedida, P.O.Box 1564, Cairo, Egypt.

³Suez University, University Road, Suez, Egypt.

Authors' contributions

This work was carried out in collaboration between all authors. Author AA has designed the study, performed and managed the statistical analysis, wrote the protocol, wrote the first draft of the manuscript and managed the submission to the journal. All authors AA, IAEM and EA have managed the literature searches, shared in writing the manuscript and read and approved the final manuscript.

Article Information

DOI: 10.9734/PSIJ/2018/46208

Editor(s):

- (1) Dr. David G. Yurth, Director of Science & Technology, The Nova Institute of Technology Holladay, Utah, USA.
(2) Dr. Roberto Oscar Aquilano, School of Exact Science, National University of Rosario (UNR), Rosario, Physics Institute (IFIR)(CONICET-UNR), Argentina.

Reviewers:

- (1) Agu Eensaar, Tallinn University of Applied Sciences, Estonia.
(2) Jūratė Sužiedelytė Visockienė, Vilnius Gediminas Technical University, Lithuania.
Complete Peer review History: <http://www.sciencedomain.org/review-history/28142>

Original Research Article

Received 07 October 2018
Accepted 26 December 2018
Published 05 January 2019

ABSTRACT

The northern coastal zone of Egypt (Mediterranean) is under the force of tension shear zones of African and European plates that generate earthquakes with variable magnitudes. We try to find a spatial relation between the collected seismic points and to evaluate how much these points affect and accelerate the frequencies of the high magnitudes' earthquakes events. Geospatial and statistical analyses (e.g. ArcGIS tools) have used to analyze nearly 3083 earthquake records in the last 65 years in the Mediterranean basin in relation to the geo-tectonic shear zones. Nearly 85% of these earthquakes were in the marine. Aegean and Anatolia shear zones are the highest contributors of the earthquakes with nearly 43% and 42% respectively. Three results of the

*Corresponding author: E-mail: aliamasha@gmail.com, ali.amasha@aast.edu;

dominant geotectonic hazards were obtained. The first is that the majority of the hot spotted earthquakes are located at the Aegean Sea which enforcing the frequency and severity of earthquakes and tsunamis than that of Anatolia plate. The northward movement rate towards the African-Aegean plate is a bit lower due to the existing of the Mediterranean ridge and Strabo and Pliny trenches which resisting the African plate northward subduction. The second is that the subsidence rates and directions at the coastal Nile delta region is aligned to the rates and directions of the tectonic plates' movements and the compaction rates of the deltaic sediments. The third is that the depths of the majority earthquakes epicenters (85%) were down to 40 km from the sea floor, one third of them were within the shallower 10 km depth. These results approve the frequencies of the severe earthquakes are potential based on the spatial statistical analysis. Therefore, the Egyptian coastal zone is vulnerability-marked where a lot of developmental activities were located.

Keywords: Geospatial analysis; geo-tectonic hazards; coastal-zone; Nile-Delta; Egypt.

1. INTRODUCTION

Natural disasters cause significant financial pressure, on government and individuals, with short-term impacts and wider long-term development implications. Vulnerability to earthquakes hazards is shifting quickly, especially in developing countries with rapid population growth, urbanization and socio-economic transformational changes. Coastal zones are known to be the most vulnerable to natural and environmental hazards due to the physical characteristics of the high flood probability, the low topography, and the high sensitivity to climatic changes, [1]. However, the deltaic environment is wealthy with natural resources that often support large populations, [2].

Earthquakes occur in the crust or upper mantle, which ranges from the earth's surface to about 800 kilometers deep (about 500 miles). However, shaking strength from an earthquake diminishes with increasing distance from the earthquake's source, [3]. Depths of earthquakes can give us important information about the Earth's structure and the tectonic setting where the earthquakes are occurring, [4]. Within continents, and along continental plate boundary transform faults, faults are only active in the shallow crust (i.e. to depths of approximately 20 km). Globally, between 1950-1999, earthquakes constituted 29% of great natural catastrophes, with 47% of the fatalities, 35% of economic losses and 18% of insured losses, [5].

Whereas, the northern coastal zone of Egypt is highly dynamic zone with various socio-economic activities and interventions, [6], the delta is potentially subjected to natural hazards including the earthquakes and probability of Tsunami.

In the context local spatial autocorrelation indices, we used the geo-statistical tools to evaluate the spatial relations between the seismic point's locations and their magnitudes' values. The local analysis methods of local Getis-Ord G_i^* statistics were used to evaluate spatial patterns of distribution of seismic magnitudes values by considering both their locations and associate correlation values. This method uses a measure known as the spatial autocorrelation coefficient to measure and test how observed locations are clustered/dispersed in space with respect to correlation values. The spatial autocorrelation at the local scale, it is necessary to calculate local autocorrelation indices like Getis-Ord G_i^* statistics, [7].

The Hot Spot Analysis by calculating Getis-Ord G_i^* statistics was performed in order to obtain more insight into how the stations with high and low levels of calculated correlation coefficients are clustered. A high positive Z-score of G_i^* statistics appears when the spatial clustering is formed by similar but high values, the larger the Z score the more intense the clustering of high values. If the spatial clustering is formed by low values, the Z-score will tend to be highly negative and the smaller the Z score is the more intense the clustering of low values. A Z-score around 0 indicates no apparent spatial association pattern, [8].

In addition, we used other geo-statistical module of the ArcGIS to compare and approve the auto-correlated values. Anselin Moran's I represents the measure of autocorrelation values that given in spatial context, [9]. Incremental Spatial Autocorrelation (ISA), which uses Moran's I measure to test for spatial autocorrelation across a series of distances throughout a study area, was conducted to determine the distance

associated with peak clustering of correlation between the analyzed seismic values. The value obtained from ISA was then used as distance threshold or radius for determining proximity weights for calculating Moran's I, [10]. The spatial econometrician which estimating the spatial autocorrelation coefficient of regression method are usual approaches, [11].

Therefore, this study primarily explores the potentiality of the current and projected risks of earthquakes. This research anticipates providing baseline information of the expected geotectonic hazards along the valuable hotspots and highly sensitive northern coastal zone of Egypt (Mediterranean coast). Priorities will include threats of, regional and national hazards of earthquakes, geological structures and faults and the susceptibility for catastrophic phenomenon such as tsunami. It is anticipated that the outcomes of this research would 1) explore the relationships between the reported seismic points within the study area based on the geo-statistical models, 2) enhance our understanding of the relationship between the tectonic plates shear zones and the seismic activities that generates the extreme geotectonic hazards, and 3) support developing hazards and

vulnerability mapping on a national and sub-regional level.

2. STUDY AREA

The study area occupies the Egyptian northern coast from Assaloum at the far west to Rafah at the far-east and extends about 40 km southward from the coastline, with a total area of about 7700 km². The area is marked by the Suez Canal at the east by and the Sinai Peninsula, from the west by the western desert, from the south by the rest of the agricultural land of the Nile delta and by the Mediterranean Sea from the north (Fig. 1). It includes big cities along the coast such as Matrouh and Alexandria to the west; Port Saeid, Al Arish and Rafah to the East and in the middle there are Damietta, Ras Albar, Baltim and Rosetta cities. The study area governed by 8 local governorates, which are; from the east to the west; north Sinai, Port Said, Al Dakahlia, Damietta, Kafr El-Shiekh, El-Beheira, Alexandria, and Matrouh. The climatic condition of this area is almost the climate of the Mediterranean Sea with minimum temperature of 10° C in winter and maximum temperature of 40° C in summer. The area is characterized by different natural landforms such as sand dunes, beaches, wetlands, and salt marshes.

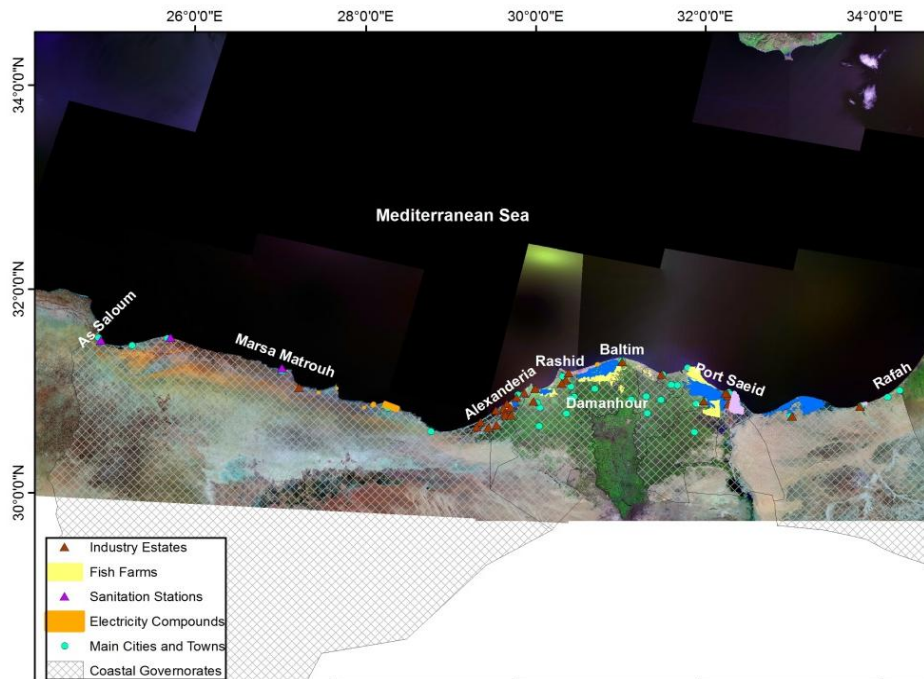


Fig. 1. Area of study of the northern coastal zone of Egypt with the major land covers features and socio-economic activities

The Mediterranean Sea is an active basin with earthquakes particularly in the area of tectonic plates; where the African plate is drifting in north direction to collide with European plates, [12]. This region is associated with numerous seismic activities of shallow and intermediate depth. However, to the east of Egypt where the Red Sea rift lies, which is a zone of plate separation along Sea-floor that has the forces pushes the African and Arabian plates apart. The zone is associated with shallow seismicity. The western side of Egypt is merely part of the African plate that is relatively stable with no major earthquake risk.

The southern Italian coastal zone, western of our study area, has been studied by Lorito et al. [13]. They estimated tsunami scenarios sources like as the large Hellenic Arc earthquake that might produce a much higher tsunami wave (up to 5 m) than those of the other source zones (up to 1.5 m). This implies that tsunami scenarios for Mediterranean Sea countries must necessarily be computed at the scale of the entire basin, (Fig. 2). The tsunami waves higher than 1 m (more than 5 m at some places) are predicted

along the northern Africa coasts. The result of edge waves, a significant energy is trapped and carried along the coast of Egypt.

Therefore, Egypt is considered as a country of low to moderate vulnerability to seismic hazard, [14]. Within the boundary of its territory, it is affected by the active tectonic structures of the rift valley of the Red Sea, Gulf of Suez and Gulf of Aqaba and other active faults within the country. Regionally, comparing the seismicity in Egypt with the large-scale tectonic features; it is recognized that two main seismic dislocation zones are bounding Egypt, 1) the Red Sea - Gulf of Suez due to NNW faults, and 2) Egypt - Mediterranean coastal dislocation zone due to deep E-W faults, [15]. These faults are responsible for some significant seismic activities and create major threat.

The focus in this research is on two main hazards sources that anticipated to potentially create major threat on the coastal zone of Egypt, 1) Geo-tectonics (earthquakes and tsunami), and 2) Land subsidence (submergence and emergence).

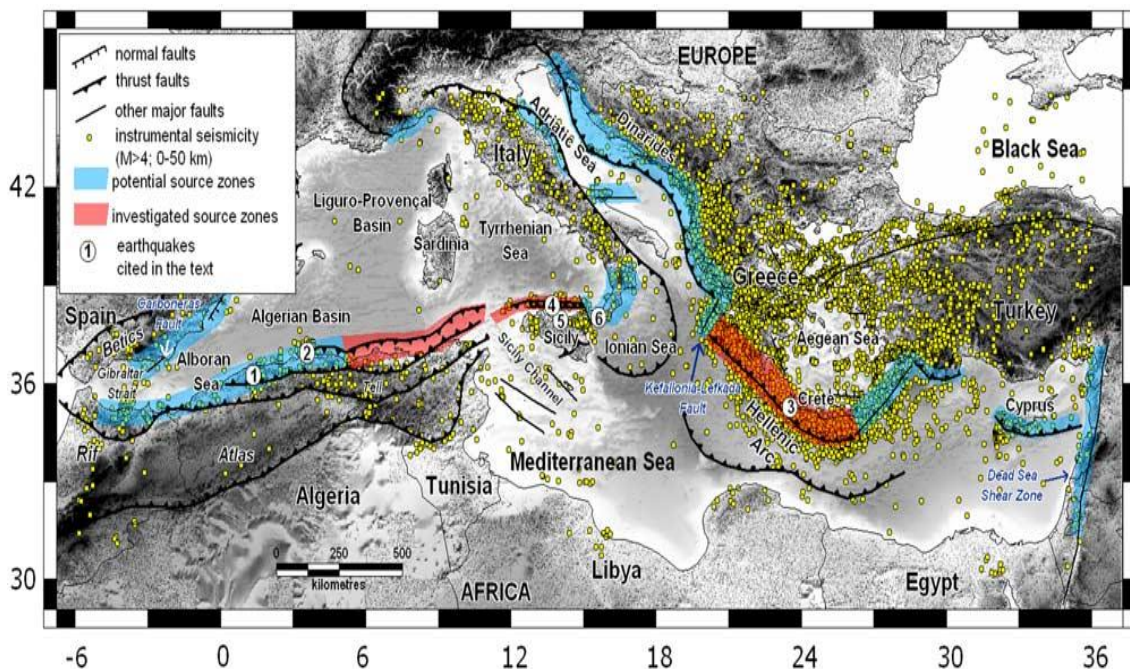


Fig. 2. Tectonic sketch map of Mediterranean basin, [13]

Instrumental seismicity (yellow dots; $M > 4$; depth 0–50 km) is taken from the ISC Catalogue (ISC, 2004). Color-shaded ribbons highlight the main structures capable of generating tsunamis that pose significant hazard to Mediterranean shore-facing settlements (shown in blue or red). Those shown in red have been investigated in this work). Selected earthquakes are shown with circles: 1) El Asnam, 1980; 2) Boumerdes, 2003; 3) Crete, 365 AD; 4) Palermo, 2002; 5) Northern Sicily, 1823; 6) Messina Straits, 1908.

3. MATERIALS AND METHODS

The data for this research were collected from various sources. The historical earthquakes data collected from the national Egyptian seismic network and USGS global earthquakes network. In addition, the geological maps, land use and land cover maps, satellite images and census data. All these data are registered into GIS platform to enable spatial analysis and mapping. Basic and advanced GIS data processing was adopted to enable for generating the required maps as follow:

- 1- Earthquakes data, as point features, with attributes of their magnitude, depth, and frequency have reached to 3083 points dated from 1951 to 2015.
- 2- Tectonic plates, as either line or polygon features, with attribute of their name and description, which used to spatially analyze their influence on the tectonic settings and relation to the earthquakes within the study area.
- 3- Land cover classes, as polygon features, that generated from classified satellite data, and used for spatial correlation with hazardous zones and estimate the natural hazards impacts on the socio-economic resources within the study area.
- 4- Population densities per the Egyptian governorates to estimate the damages and losses.

In this context, we used different modules of the ArcGIS Desktop 10.2 Software for data processing, analysis and mapping of the gathered data, as follow:

- 1- The ArcMap module used for data entry and editing to integrate all the collected seismic data in one layer.
- 2- The earthquakes' points were processed and analyzed by the ArcGIS modules as follow:
 - a. The First Module is The Spatial Statistical Tools / Mapping clusters / Optimized Hot Spot Analysis. This module executes the Optimized Hot Spot Analysis (Getis-Ord G_i^*) tool using parameters derived from characteristics of the earthquakes' magnitudes as incident points. It interrogates the data to obtain the settings that will yield optimal hot spot results. If, for example, the Input Features dataset contains incident point data, the tool will aggregate the incidents

into weighted features. Using the distribution of the weighted features, the tool will identify an appropriate scale of analysis.

Since the Optimized Hot Spot Analysis tool uses the average and the median nearest neighbor calculations for aggregation and also to identify an appropriate scale of analysis, the Initial Data Assessment component of the tool will also identify any locational outliers in the Input Features or Polygons For Aggregating Incidents Into Points and will report the number it encounters. To do this, the tool computes each feature's average nearest neighbor distance and evaluates the distribution of all of these distances. Features that are more than a three standard deviation distance away from their closest non-coincident neighbor are considered locational outliers.

The statistical significance of the output features will be automatically adjusted for multiple testing and spatial dependence using the False Discovery Rate (FDR) correction method. Also, the output features will reflect the aggregated weighted features (fishnet polygon cells, the aggregation polygons you provided for the Polygons for Aggregating Incidents into points parameter, or weighted points). Each feature will have a z-score, p-value, and G_i _Bin result, [16].

The output of this module is classified as – cold spot confidence (99, 95, and 90%) and the hot spot confidence (90, 95, and 99%).

- b. The data is also processed by the module “Spatial Statistics Tools / Rendering / Cluster/Outlier Analysis with Rendering”. The Cluster and Outlier Analysis tool identifies spatial clusters of features with high or low values and spatial outliers. To do this, the tool calculates a local Moran's “I” value, a z-score, a p-value, and a code representing the cluster type for each statistically significant feature. The z-scores and p-values represent the statistical significance of the computed index values. Positive values for “I” indicates that a feature has neighboring features with similarly high or low attribute values; this feature is part of a cluster. A negative value for “I” indicates that a feature has neighboring features with dissimilar values; this feature is an outlier. In either instance, the p-value for

the feature must be small enough for the cluster or outlier to be considered statistically significant. The output cluster/outlier type (COType) field distinguishes between a statistically significant cluster of high values (HH), cluster of low values (LL), outlier in which a high value is surrounded primarily by low values (HL), and outlier in which a low value is surrounded primarily by high values (LH). Statistical significance is set at the 95 percent confidence level. When no FDR correction is applied, features with p-values smaller than 0.05 are considered statistically significant. The FDR correction reduces this p-value threshold from 0.05 to a value that better reflects the 95 percent confidence level given multiple testing.

The Cluster/Outlier Analysis with Rendering tool combines the Clusters and Outlier Analysis and ZScore Rendering tools in a model. It gives a set of weighted features, identifies hot spots, cold spots, and spatial outliers using the Anselin Local Moran's I statistic. Then, it applies cold-to-hot rendering to the z-score results, [16].

- c. The third module is the Geo-statistical Analysis Tools / Interpolation / Kernel Interpolation with Barriers. The Kernel Interpolation is a variant of a first-order Local Polynomial Interpolation in which instability in the calculations is prevented using a method similar to the one used in the ridge regression to estimate the regression coefficients. When the estimate has only a small bias and is much more precise than an unbiased estimator, it may well be the preferred estimator. The Kernel Interpolation model uses the shortest distance between points so that points on the sides of the specified nontransparent (absolute) barrier are connected by a series of straight lines.

The Local Polynomial Interpolation prediction error is estimated assuming that the model is correct. This assumption is often violated and the spatial condition number highlights areas where the predictions and prediction standard errors are unstable. In the Kernel Smoothing model, the problem with unduly large prediction standard errors and questionable predictions is corrected with the ridge parameter by introducing a small amount of bias to the equations. Since the ridge

parameter introduces bias in order to stabilize the predictions, the ridge parameter should be as small as possible while still maintaining model stability, [16].

This module uses the locations of earthquakes' magnitudes as points and the lines of tectonic plates as input layers to find a kind of relation between the intensity/magnitude values with the tectonic plates sheer zones.

- 3- The ArcMap module is used also for mapping the outputs of the processed data.

4. RESULTS AND DISCUSSION

4.1 Vulnerability to Geotectonic Hazards

Egypt is located in the southeastern part of the Mediterranean Sea, and represents a subordinate part of the Eastern Mediterranean region, which is a small ocean basin known by its unusual tectonic complexity. It includes a short segment of the convergence boundary between Africa and Eurasia creating northward movement of the African Plate relative to the Eurasian Plate, [17-19]. Subduction in this segment is along two very small arcs, the Hellenic and Cyprean arcs. The risk of earthquakes is anticipated to be at highest level in the Egyptian Delta region due to the dense concentration of population and human economic development, [12].

Locally, Sinai triple junction region, which occur in a NW trend closely parallel to the Gulf of Suez, is characterized by intense seismicity associated with complex tectonic activity of three plates. The total reported earthquakes during the same time span are about 52 events with a maximum magnitude of 6.3 and about 49 events with minimum magnitude of 3.1 and maximum of 5.9 Richter scale, [20,21].

Unfortunately, most of the well recorded earthquakes are land sources, with no insights on the marine large number of earthquakes reported from the Mediterranean Basin. The Arabian-Agean Plates are significantly contributed to these earthquakes that might create Tsunami. Two old incidents of Tsunami were recorded in Egypt due to these tectonic plates, which were in the years 320 and 1303 and caused severe damage to Alexandria, [22] and [23]. The event of the year 320 was very destructive that destroyed more than 50,000

houses (one third of the city) and killed 5,000 people in Alexandria, [24].

To evaluate the magnitude of geotectonic hazards from marine earthquakes that might create Tsunami, it is important to map the location of earthquakes in relation to the plates' zones and the coastal zone of Egypt as well. (Fig. 3) shows the spatial distribution of both land and marine earthquakes since 1951 till 2015 in the Mediterranean Basin in relation to the geotectonic shear zones. It was found that 85% of

these earthquakes are located in the marine. In addition, Aegean and Anatolia shear zones is the highest contributor of the earthquakes with nearly 43% and 42% respectively. However the least one is the Arabia zone with 1%, and Africa is about 14%, (Table 1).

The shallower earthquakes' activities in the Hellenic arc are higher frequency than in the Cyprian arc, which extends from Albania in the west to southwestern Turkey in the east. About 85% of the earthquakes epicenters were less

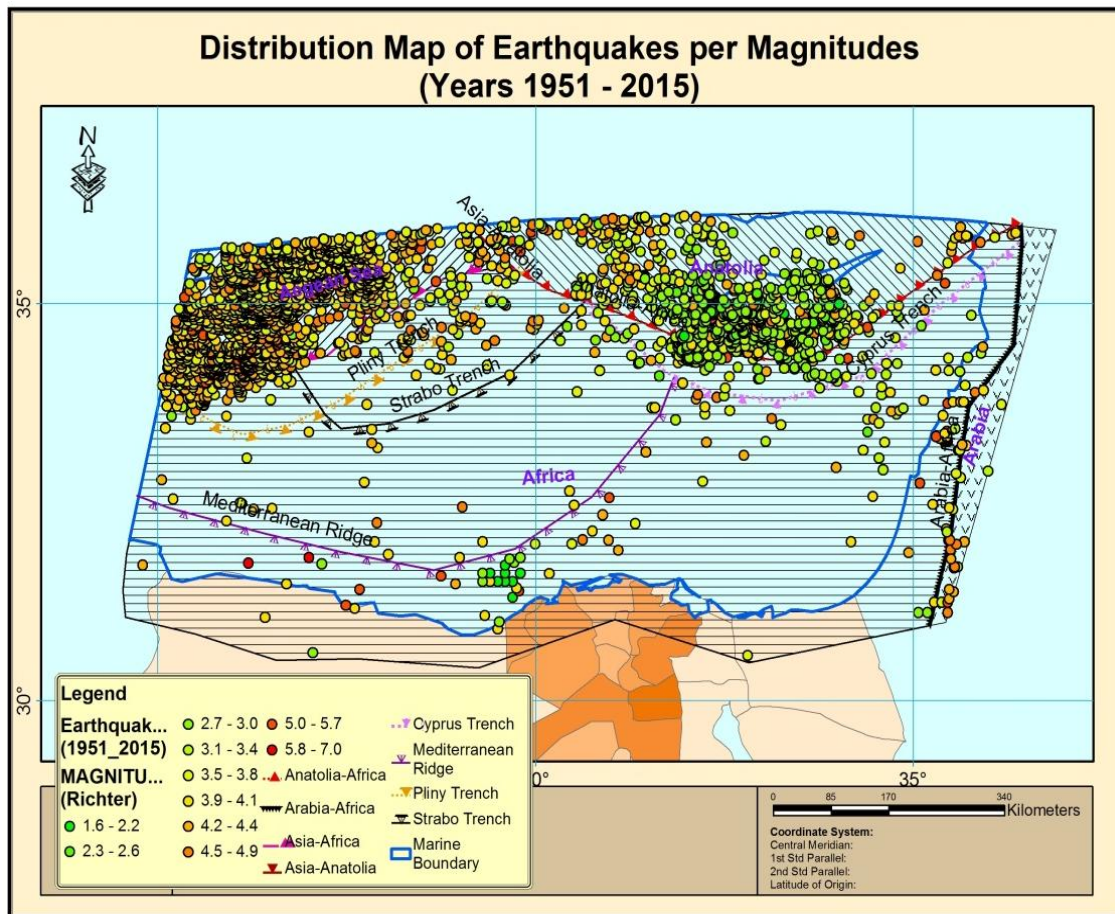


Fig. 3. Spatial distribution of the earthquakes points (1951-2015) and the tectonic plates along the coastal and marine of the study area

Table 1. Statistics of the earthquakes and the tectonic plates within the Mediterranean

Source	Number	%	Tectonic Zone	Number	%
Marine	2618	85%	Aegean Sea	1321	43
Land	465	15%	Anatolia	1297	42
			Africa	442	14
			Arabia	23	1
Total	3083	100%		3083	100

than or equal 40 kilometers beneath the sea floor, whereas nearly one third of the analyzed earthquakes depths were less than or equal 10 kilometers, Table 2. These activities are mostly seaward that are potential for creating Tsunami, Fig. 4. Moreover the southern part of the Aegean Sea is moving as a relatively rigid block compared with the surrounding zones, [25].

Table 2. Summary Statistics of the analyzed Earthquakes Depths

Depth (meters)	Earthquakes No.	%
0 - 10	844	27.38
11 - 20	356	11.55
21 - 30	575	18.65
31 - 40	828	26.86
41 - 50	136	4.41
51 - 191	344	11.16
Total	3083	100

Several statistics in the Spatial Statistics toolbox are inferential spatial pattern analysis techniques including Spatial Autocorrelation (Global Moran's

I), Cluster and Outlier Analysis (Anselin Local Moran's I), and Hot Spot Analysis (Getis-Ord Gi). A positive value for I indicate that a feature has neighboring features with similarly high or low attributes values; this feature is part of a cluster. A negative value for I indicates that a feature has neighboring features with dissimilar values; this feature is an outlier. However, the positive results of Moran's I statistic with significant p-values and high Z-scores indicate spatially clustered data sets. At the same time, negative Moran's I depicts that the spatial pattern is more spatially dispersed [26; 27].

The Spatial Autocorrelation (Global Moran's I) tool measures spatial autocorrelation based on both feature locations and feature values simultaneously. Given a set of features and an associated attribute, it evaluates whether the pattern expressed is clustered, dispersed, or random [27]. The Spatial Autocorrelation (Global Moran's I) was used in relation to the correlated points where the seismic points as the current study.

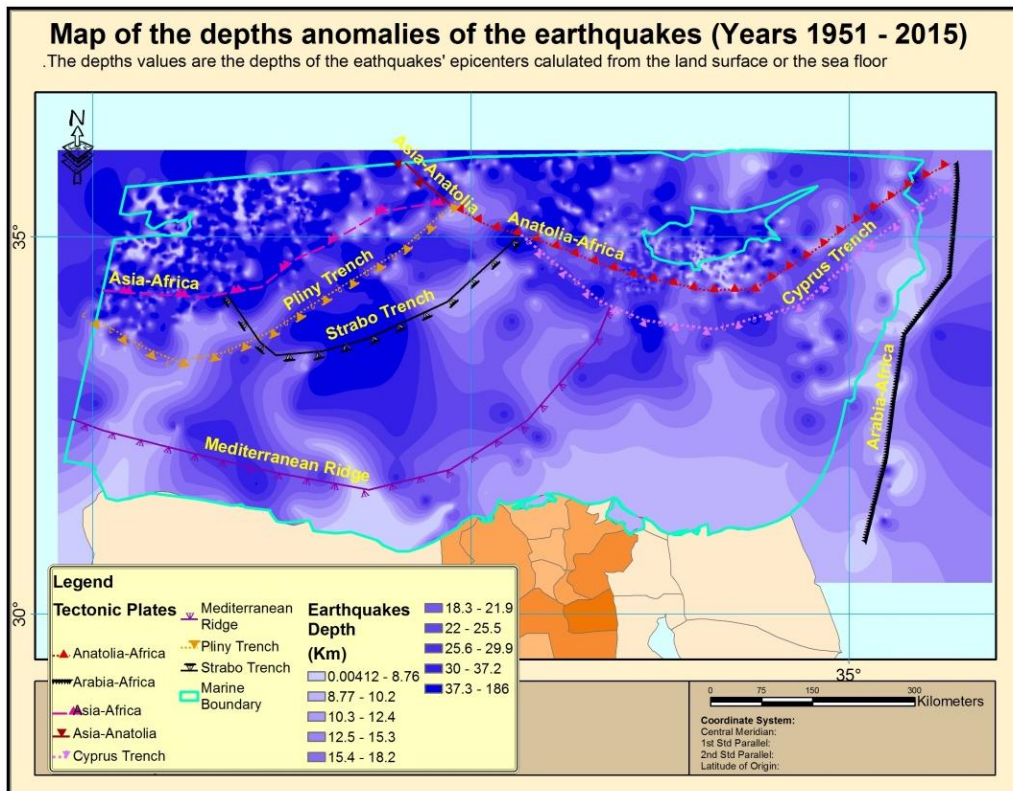


Fig. 4. The depths anomalies of the earthquakes within the tectonic plates

To map the clusters by the spatial statistical tools, the Getis-Ord G_i^* analysis on the distribution of the earthquakes' magnitudes, it optimized hot spot areas that clearly show the highest number and effectiveness of earthquakes are located at the Aegean Sea plate. The majorities of the hot spotted earthquakes are spatially concentrated within the Aegean Sea plate and to the southern margin of the Mediterranean ridge, while the majority of the cold spotted ones are at the Anatolia Plate, (Fig. 5).

In addition, throughout the statistical analysis of the optimized hot spot of the G_i^* values, the hot spot points (90, 95 and 99%) calculated as 44% of the total processed points were 3083, (Table 3). Based on the distributions of these values, this explains that the earthquakes at the Aegean Sea plate and the areas along the Mediterranean ridge are might potential source of the massive and frequent shakes and tsunamis.

High/low clustering (Getis-Ord G_i) or cluster-outlier analysis (Anselin Local Moran's I) statistics; the term hot spot has become an integral part of the study called data analysis and is popular with most of the analyst. A hot spot as the name suggests is a state of indicating some subjects of clusters in a spatial distribution [28;29]. The cluster/outlier type field distinguishes between a statistically significant cluster of high values (HH), cluster of low values (LL), outlier in which a high value is surrounded primarily by low values (HL), and outlier in which a low value is surrounded primarily by high values (LH). Statistical significance is set at the 95 percent confidence level. For statistically significant positive z-scores, the larger the z-score, the more intense the clustering of high values (hot spot) [30;31].

Therefore, when applying the Cluster-Outlier Analysis with Rendering which uses the Anselin Local Moran's I statistics, it shows that the high-high clusters and low-high outliers spots (low earthquakes surrounded by high ones) are dominated at the Aegean Sea plate. While, the high-low outlier spots (high earthquakes surrounded by low ones) and low-low cluster spots are dominated at the Anatolia Plate, (Fig. 6). Throughout the statistical analysis of the cluster-outlier analysis with rendering result, the high-high clusters and high-low outliers' sums to 44% of the total analyzed points were 3083, (Table 4). This result is extremely similar to the

result of optimized hot spot analysis and approves the same findings.

In this context, we try to find a relation between the seismic activities and the sheer zones of the named tectonic plates, ridges and trenches, a kernel interpolation with barriers of the geo-statistical analysis tools module was used. The higher magnitudes of earthquakes (considered to ≥ 3.9 in Richter scale) were dominated to the western side of the African plate especially at the Aegean Sea and Asian-African sheer zone and to the south of the Mediterranean Ridge and southeast of the Arabian-Asian sheer zone. It is extremely the same conclusion of the above analyses, the high-high clusters and high-low outliers of the Cluster-Outlier Analysis with Rendering and the hot spots of the optimized hot spot analysis. Therefore, the potentiality of the frequent and massive earthquakes and tsunami phenomena might happen at the mentioned zones, (Fig. 7).

4.2 Land Subsidence – Submergence

The Nile Delta is geologically created as a deep graben that filled with thick column of clay and fine sediments. Few researches recognized the difference in the land subsidence along the Nile Delta coast founding that the eastern region is higher than the west. They also anticipated that the land subsidence in the Nile Delta is due to the compaction of sediments. The difference of the land subsidence rates of the northern Nile delta is not only referred to the sediments' compaction that stated by Stanley and Warne [32]; and Frihy [33], but also it may be varied due to the differential rates of the African plate northward movements from the west to the east. This variation is previously stated by Stanley [34] and Stanley [35] due to differential compaction and varying thicknesses in the Holocene layers. Stanley and Clemente [36] summarizes the land subsidence rate of the Nile delta coastal zone as about 3.7 mm/yr in the NW delta, about 7.7 mm/yr in the N delta, and about 8.4 mm/yr in the NE delta, based on compaction rates of Holocene sediments' thicknesses which decreases from the east to the west.

Furthermore, to the east and based on age-dated sediment core sections, [32] and [35] have estimated long-term average subsidence rates across the Nile delta region. The processes of compaction and dewatering of the thick accumulated deposits of fluvio-marine deltaic mud sequence formed in the Holocene have

induced higher rates of subsidence ranging from 5 mm/yr at Port Said in the east, where the deltaic plain thickness is about 50 meter, to 1 mm/yr further to the west, where the deltaic plain thickness is decreased or nearly absent below Alexandria coastal plain, [32,37], (Fig. 8).

Table 3. Summary of the Optimized Hot Spot Analysis (Getis-Ord Gi*)

Optimized Hot Spot Analysis (Getis-Ord Gi*)	Gi_Bin	Count Gi_Bin	%
Cold Spot - 99% Confidence	-3	1148	37.24
Cold Spot - 95% Confidence	-2	52	1.69
Cold Spot - 90% Confidence	-1	13	0.42
Not Significant	0	486	15.76
Hot Spot - 90% Confidence	1	96	3.11
Hot Spot - 95% Confidence	2	187	6.07
Hot Spot - 99% Confidence	3	1101	35.71
Total		3083	100

Table 4. Summary of the Cluster_Outlier Analysis with Rendering

Cluster/Outlier with Rendering	Count COType	%
Not Significant	589	19.10
High-High	1035	33.57
High-Low	342	11.09
Low-High	140	4.54
Low-Low	977	31.69
Total	3083	100

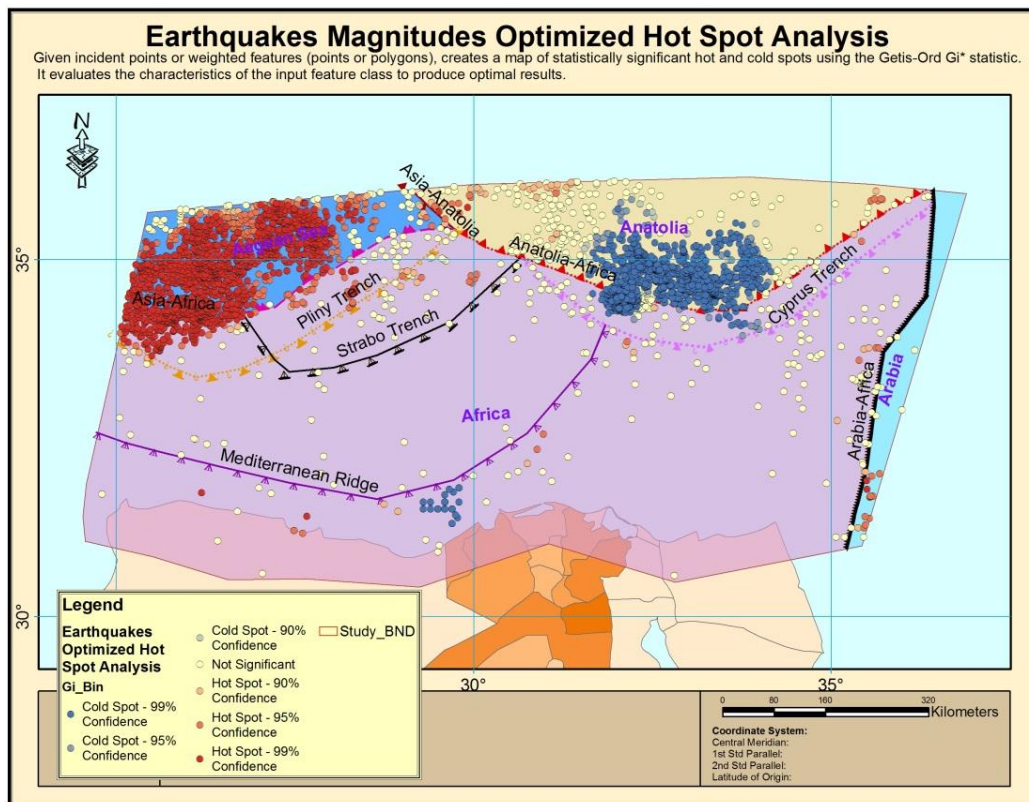


Fig. 5. Spatial statistical mapping of the earthquakes' magnitudes by Hot Spot Analysis (Getis-Ord Gi*)

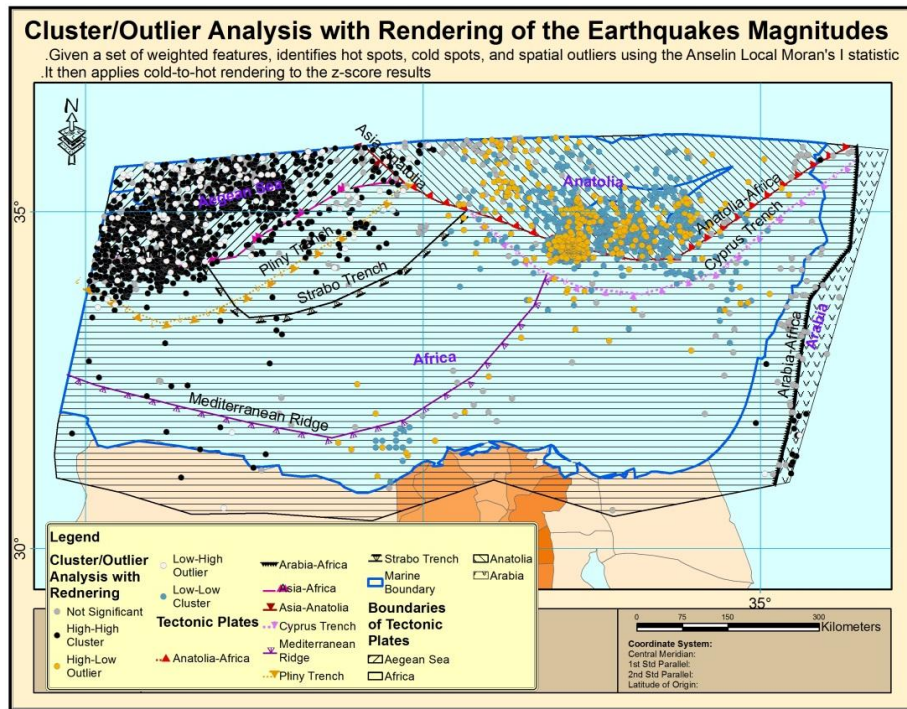


Fig. 6. Spatial statistical mapping of the earthquakes by Cluster-Outlier Analysis with Rendering

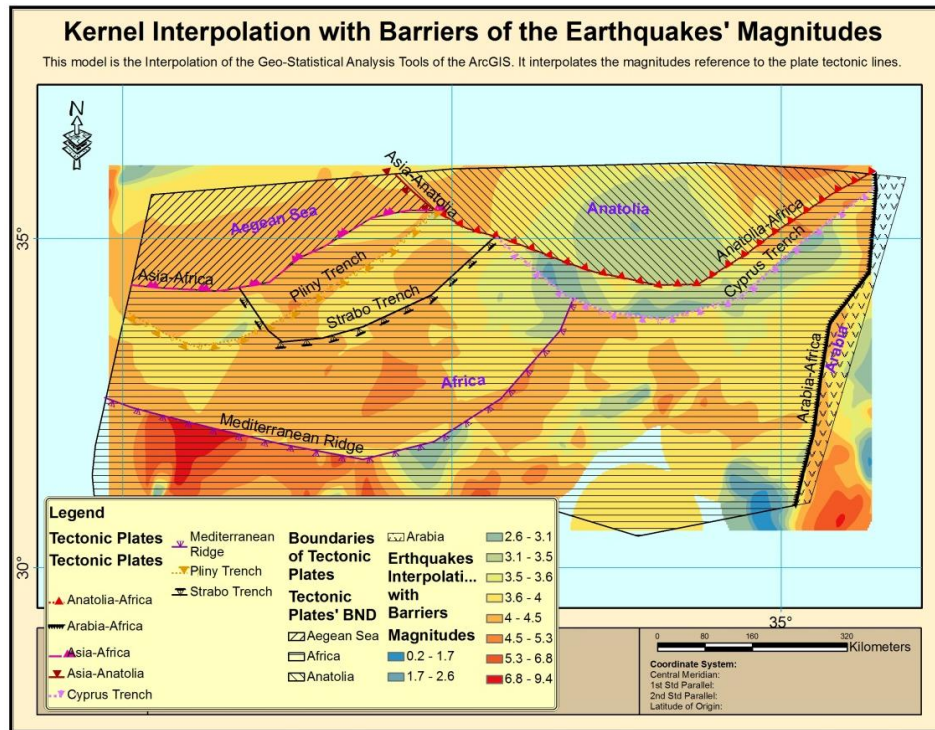


Fig. 7. Kernel interpolation of the earthquakes' magnitudes with barriers of plate tectonics' shear zones

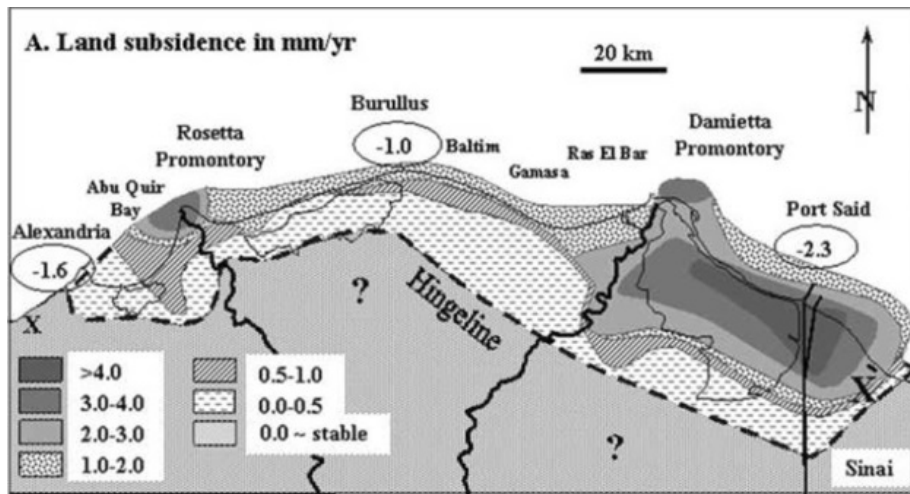


Fig. 8. Spatial distribution of land subsidence rates in the northern delta
 Source: modified from [21]

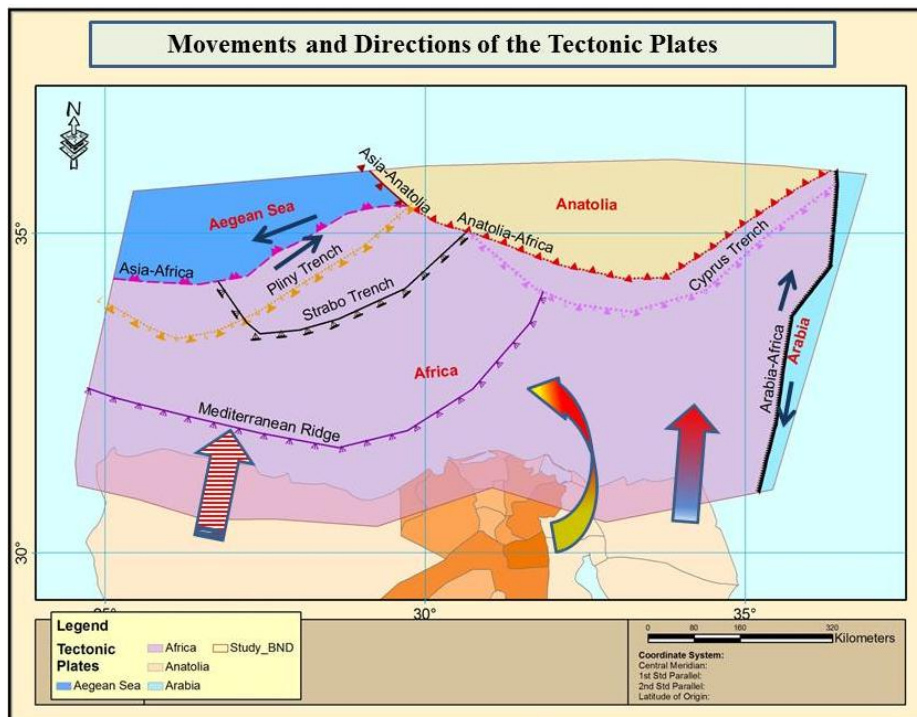


Fig. 9. Expected directions of the plate tectonics' movements within the study area

The variability of emergence and subsidence of Alexandria land (ranging between -5 mm and $+7$ mm per year) as calculated by Warne and Stanley [38] may be attributed to the impact of tectonic activities. Tectonic activities in Alexandria have been recorded from the observations on submerged Roman and Greek ruins in the Eastern harbor and Abu Quir Bay, as old as 2,500 years had submerged from 2 to 5.5 m, [38] and [39]. Therefore, the Hellenistic city of

Canopus (500 BC) in Abu Quir Bay was originally located 3 m above sea level, which may imply that it has submerged of 8 m during the past 2,500 years.

To summarize this, we founds that the driving forces influence the subsidence of the Nile delta coastal zone is varied from the west, where the geo-tectonic-controlled, to the east, where the delta sediments compaction. We propose that

land subsidence is not only due to the compaction of the Nile delta grapsen's sediments (if this is the case the rate of the subsidence should be similar along the Nile Delta), it is driven by geo-tectonics. The differential movement of the African plate is also generates the differential sea waves and tidal gauges as well. In this case, the sea level rise potentiality is a result of the subduction movements of the African, Agean and Arabian tectonic plates. This align with [40,41], where the structure framework controlling the vertical motion due to the geodynamic setting including earthquakes epicenters and major active fault trends were detected at the north western Nile delta. The structural pattern results from a complex interplay of fault trends of the N-S faults (Abu Quir), NE faults (Rosetta), NW Suez-Cairo-Alexandria line, and NE-SW (Qattara-Eratosthenes line). These structural trends indicate that the main cause of subsidence in the western Nile delta is ongoing faulting, as well as down warping, of the underlying 3000 meters of Late Miocene to Quaternary sequences.

In addition, the depths of the majority earthquakes epicenters (85%) were above 40 kilometers from the sea floor, one third of them were down to 10 kilometers depth. (Fig. 9) summarizes the predicted directions of the plate tectonic movements based on the geospatial analysis and findings of this research. At the African plate, the movement of the eastern side is increased northward along the Arabian-African shear zone (at eastern Nile delta and Sinai). Also, the movement of the western side of the African plate is north-northeast at the western desert of Egypt while it is skewed to the north-northwest along the eastern coastal zone of the Nile delta. This makes the movement along the eastern coastal zone is higher than the western coastal zone of the Nile delta.

5. CONCLUSION

Geo-spatial and statistical analysis found to be a potential tool to show off the spatial relation between the seismic activities and the tectonic plates within the area of study. The Egyptian coast that is a part of the African plate and extended to the Aegean plate is dissected by the Mediterranean Ridge, Strabo Trench and Pliny trench. There are three predicted scenarios:

1. The majority of the hot spotted earthquakes are located at the Aegean

Sea due to the named ridges/trenches which make the frequency and severity of earthquakes than that of Anatolia plate. This makes the northward movement rate towards the Aegean-African plate is a bit lower due to named ridges/trenches making a resistance to the African plate northward subduction than that to the eastern Mediterranean side where only the Cyprus trench exists.

2. The subsidence rates aligned to the rates of the tectonic plates' movement in addition to the coastal deltaic sediments compaction. This was aligned with the results from the kernel interpolation of the seismic points and their relations with the boundaries of the plates' shear zones.
3. As the result of the cluster-outlier analysis with rendering, there are about 44% of High-High and High-Low relations. This proves that some of the points may generated/accelerated the most severe earthquakes due to geospatial statistical relations that happened between the H-H and H-L seismic points. This also approved by the hot spot analysis that results about 44% of the sum the hot spot (90-95-99%) confidence points.

COMPETING INTERESTS

Authors have declared that no competing interests exist.

REFERENCES

1. Milliman JD, Qin YS, Park YA. Sediment and sedimentary processes in the Yellow and East China Seas A. Taira, F. Masuda (Eds.), *Sedimentary Facies in the Active Plate Margin*Terra Scientific, Tokyo. 1989; 233–249.
2. Syvitski JPM, Saito Y. Morphodynamics of deltas under the influence of humans *Global Planet. Changes.* 2007;57:261–282.
3. Gavin Hayes & Tony Crone, United States Geological Survey (USGS). Available:https://www.usgs.gov/faqs/what-depth-do-earthquakes-occur-what-significance-depth?qt-news_science_products=0#qt-news_science_products (26th Sep. 2018)
4. Petrishchevsky M. The relation of seismicity to lithospheric density inhomogeneities in the Russian Far East,

- Journal of Volcanology and Seismology. 2007;1(6):410–420.
5. Munich Re. Topics geo annual review: Natural catastrophes 2006. Geo Risks Research. Munich Re Group, Munich; 2006.
 6. Abou El-Magd I, Hermas EA. Human impact on the coastal landforms in the area between gamasa and kitchner drains, Northern Nile Delta, Egypt J. Coastal Res. 2010;26(3):541–548.
 7. Getis A, Ord JK. The analysis of spatial association by use of distance statistics. *Geographical Analysis*. 1992;24(3):189–206.
 8. Wong DWS, Lee J. Statistical analysis of geographic information with ArcView GIS and ArcGIS. John Wiley & Sons, Hoboken, NJ, USA; 2005.
 9. O’Sullivan D, Unwin DJ. Geographic information analysis. John Wiley & Sons; 2003.
 10. ESRI. Spatial Statistics Tools, ArcMap 10.1. ESRI, Redlands, California; 2012.
 11. Anselin L. Spatial econometrics: Methods and models. Dordrecht: Kluwer; 1988.
 12. Degg MR, Doornkamp A. Earthquake hazards atlas, 2 - Egypt based on the R. O. An Earthquake hazard zonation scheme R. O. A Reinsurance Office Association Aldernary House, Queen Street, London EC 4N 1ST, United Kingdom, P- CL; 2.1. - C 1. 2.24; 1990.
 13. Lorito S, Tiberti MM, Basili R, Piatanesi A, Valensise G. Earthquake-generated tsunamis in the Mediterranean Sea: Scenarios of potential threats to Southern Italy. *J. Geophysical. Research*. 2008;113: B01301.
DOI: 10.1029/2007JB004943
 14. El-Sayed AR, Wahlstrom Kulhanek O. Seismic hazard of Egypt. *Natural Hazards*. 1994;10:247-260.
 15. Maamoun ME, Ibrahim EM. Tectonic activity in Egypt as indicated by earthquakes. *Acadmy of Scientific Research and Technology, Helwan Institute of Astronomy and Geophysics*. 1978;Bull No. 170:20.
 16. Esri, ArcGIS Desktop 10.2 Help.
 17. Rabinowitz P. and Ryan W. Gravity anomalies and crustal shortening in the Eastern Mediterranean. *Tectonophysics*. 1970;5–6:585– 608.
 18. Taymaz T, Jackson J, Westaway R. Earthquake mechanism in the Hellenic trench near Crete. *Geophysics. Journal Int*. 1990;102:695–731.
 19. Abou Elenean K. Seismotectonics of the Mediterranean region north of Egypt and Libya, M. Sc. Thesis. Fac. of Sci., Mansoura Univ., Egypt. 1993; 198.
 20. Badawy A. Earthquake hazard analysis in northern Egypt *Acta Geod. Geophys. Hung*. 1998;33:341–357.
 21. Badawy A, Al-Gabry M, Girgis M. Historical seismicity of Egypt. In: A Study for Previous Catalogues Producing Revised Weighted Catalogue the Second Arab Conference for Astronomy and Geophysics, Egypt; 2010.
 22. Ambraseys NN, Melville CP, Adams RD. The seismicity of Egypt, Arabia and the Red Sea. Cambridge University Press, Cambridge. 1994;182.
 23. El-Sayed A, Vaccari F, PANZA G. Deterministic seismic hazard in Egypt, *Geophys. J. Internat*. 2001;14:555–567.
 24. El-Sayed A, Korrat I, Hussein HM. Seismicity and seismic hazard in Alexandria (Egypt) and its surroundings. *Pure appl. Geophysics*. 2004;161:1003–1019.
DOI: 10.1007/s00024-003-2488-8.
 25. McKenzie D. Some remarks on the development of sedimentary basins. *Earth and Planet Science Letters*. 1978;40:25–32.
 26. Luković J, Blagojević D, Kilibarda M, Bajat B. Spatial pattern of North Atlantic oscillation impact on rainfall in Serbia. *Spatial Statistics Journal*. 2015;14:39–52. Available:<http://dx.doi.org/10.1016/j.spasta.2015.04.007>
 27. ESRI, Spatial statistics tools, ArcMap 10.3. ESRI, Redlands, California. ESRI, ArcMap 10.3. ESRI, Redlands, California; 2014.
 28. Ansari SM., Kale K. Methods for crime analysis using GIS. ESRI; 2014. Available:www.esri.com/publicsafety
 29. ESRI. The use of ArcGIS Geostatistical analyst exploratory spatial data analysis. (Accessed 20th Dec. 2018) Available:http://dusk2.geo.orst.edu/gis/geo_stat_analyst.pdf
 30. Zhou W, Minnick MD, Mattson ED, Geza M, Murray KE: GIS-based geospatial infrastructure of water resource assessment for supporting oil shale development in Piceance Basin of Northwestern Colorado. *Computers & Geosci*. 2015;77:44-53.

31. Mahboubi P, Parkes M, Stephen C, Chan HM. Using expert informed GIS to locate important marine social-ecological hotspots. *Journal of Environmental Management*. 2015;160:342-352. Available:<http://dx.doi.org/10.1016/j.jenvman.2015.03.055>
32. Stanley DJ, Warne AG. Nile Delta: Recent geological evolution and human impact. *Science, New Series*. 1993;260(5108):628-634. Available:<https://www.jstor.org/stable/2881247>
33. Frihy OF. The Nile delta-Alexandria coast: Vulnerability to Sea-level rise, consequences and adaptation. *Mitigation and Adaptation Strategies for Global Change*. 2003;8(2):115-138.
34. Stanley DJ. Subsidence in the northeastern Nile delta: Rapid rates, possible causes, and consequences. *Science*. 1988;240:497-500.
35. Stanley DJ. Recent subsidence and northeast tilting of the Nile delta, Egypt", *Marine Geology*. 1990;94(1-2):147-154. Available:[http://dx.doi.org/10.1016/0025-3227\(90\)90108-V](http://dx.doi.org/10.1016/0025-3227(90)90108-V)
36. Stanley DJ, Clemente PL. Increased land subsidence and sea-level rise are submerging Egypt's Nile Delta Coastal Margin"; *GSA Today*. 2016;27. Available:<http://dx.doi.org/10.1130/GSATG312A.1>.
37. Chen Z, Warne AG, Stanley DJ Late Quaternary evolution of the northwest Nile delta between Rosetta and Alexandria, Egypt. *J. Coastal Research*. 1992;8:527-561.
38. Warne AG, Stanley DJ. Late quaternary evolution of the North West Nile delta and adjacent coast in the Alexandria region Egypt", *Journal of Coastal Research*. 1993;9:26-64.
39. El Sayed MKh Sea level rise in Alexandria during the late Holocene: archaeological evidences. *Rapp Comm Int Mer Me'diterrane'e*; 1988.
40. Garziglia S, Migeon S, Ducassou E, Loncke L, Mascle J. Mass-transport deposits on the Rosetta province (NW Nile deep-sea turbidity system, Egyptian margin): Characteristics, distribution, and potential causal processes. *Marine Geology*. 2008;250:180-198. Available:<http://dx.doi.org/10.1016/j.margeo.2008.01.016>
41. Zaghoul ZA, Elgamal MM, El Araby H, Abdel Wahab W. Evidences of neotectonics and ground motions in the northern Nile Delta', in Z.M. Zaghoul' and M.M. Elgamal (eds.), *Deltas-Modern and Ancient, Egypt*, proceedings of Mansoura University, First International Symposium on the Deltas. 1999;285-314.

© 2018 Amasha et al.; This is an Open Access article distributed under the terms of the Creative Commons Attribution License (<http://creativecommons.org/licenses/by/4.0>), which permits unrestricted use, distribution, and reproduction in any medium, provided the original work is properly cited.

Peer-review history:
The peer review history for this paper can be accessed here:
<http://www.sciencedomain.org/review-history/28142>